

## Phase equilibria in mesoporous materials

Michael Steiger, Kirsten Linnow

University of Hamburg, Department of Chemistry, Inorganic and Applied Chemistry

### Summary

Phase equilibria in mesoporous materials are affected by the curvature of the vapor–solution and the crystal–solution interfaces. The present paper provides a discussion of the thermodynamic treatment of these influences in unsaturated small pores including equations for the calculation of vapor–liquid and solid–liquid phase equilibria. These equations are used together with an electrolyte solution model to predict the solubilities, freezing temperatures and saturation humidities of NaCl solutions in porous materials with different pore sizes. While there is a strong influence of pore size on the freezing temperature of the solvent and the saturation humidity, the influence on the solubility is less pronounced due to a partial compensating effect of the increased solubility of small crystals and the solubility decrease under conditions of low pressure as in unsaturated nanosized pores. It is also shown that the same model equations can be applied to predict the behavior of aerosol nanoparticles.

*Keywords: mesoporous materials, crystal size, pressure, unsaturated materials, interfacial energies, solubility calculation, nanoparticles*

### 1 Introduction

The pressure generated by crystal growth of salts in confined spaces of porous building materials such as stone, brick and concrete is generally recognized as a major cause of damage in ancient monuments and modern buildings. Crystal growth is also considered as an important weathering mechanism of natural rocks in a variety of environments not only on earth, e.g. in deserts, dry Antarctic valleys and tropical coastlines, but also on Mars. Crystal growth in porous materials is the result of phase changes that are induced by variation of ambient temperature and relative humidity, RH. Unfavorable conditions of temperature and RH may result in repeated cycles of freezing–thawing, crystallization–deliquescence and hydration–dehydration, respectively. Under such conditions, building materials and natural rocks are subject to rapid decay. The relevant phase equilibria in building materials can be modeled using a multi-component electrolyte solution model such as the model presented in the previous chapter [1]. It is then possible to predict ambient conditions, i.e. temperature and relative humidity that minimize the frequency of occurrence of undesired phase changes inducing crystal growth in por

---

ous materials. For instance, model simulations are particularly helpful to predict the influence of changes in the room climate to salt contaminated masonry [2].

The range of pore sizes found in various building materials extends from a few nanometers to hundreds of micrometers and it is important to consider possible effects of pore size on the various phase equilibria in these materials. Following the recommendations of IUPAC [3] pores with pore diameters exceeding about 50 nm are called macropores, while pores with diameters between 2 nm and 50 nm are called mesopores, and even smaller pores are called micropores. There is no restriction for the application of electrolyte solutions models and the calculation of phase equilibria in macroporous materials. However, in the small pores of mesoporous materials the situation becomes more complicated as the influence of interfaces can no longer be neglected. Such small pores are commonly found in concrete and sometimes in bricks and fine-grained natural stone materials. Phase equilibria in mesoporous materials are strongly affected by both the vapor–solution and the crystal–solution interfaces. Firstly, the available pore space limits the maximum size of growing crystals and the interfacial energy of the crystal–liquid interface affects the solubility of dissolved species [4]. Secondly, in an unsaturated porous material, a curved liquid–vapor interface is formed resulting in a substantial pressure decrease. Hence, in addition to crystal size effects the influence of low pressure on the various phase equilibria has to be considered. The present paper provides a discussion of the thermodynamic treatment of phase equilibria in unsaturated small pores including the vapor–liquid equilibrium, freezing temperatures and salt solubilities.

## 2. Theoretical background

### 2.1 Unsaturated porous materials

Phase equilibria in mesoporous materials are affected by the vapor–solution and the crystal–solution interface. Figure 1 depicts the situation of a crystal growing in idealized pores of cylindrical geometry. Considering a liquid in a porous material, it is important to distinguish the degree of saturation which is defined as the fraction of the pore space filled with liquid water. In a saturated material the liquid–vapor interface is flat (Fig. 1a) while, in an unsaturated porous material, a curved liquid–vapor interface is formed. For a wetting fluid such as in the case of water in building materials, the curvature of the liquid–vapor interface is concave as illustrated in Fig 1b. The curvature of the interface results in a pressure drop which is given by Laplace's law:

$$\Delta p = p_l - p_a = 2\gamma_{lv}/r_{lv} = -2\gamma_{lv} \cos \theta / r_p \quad (1)$$

Here,  $p_l$  is the pressure in the liquid phase,  $p_a$  is the ambient pressure,  $\gamma_{lv}$  and  $r_{lv}$  are the interfacial energy and the radius of curvature of the liquid–vapor interface,  $\theta$  is the contact angle of water with the pore walls and  $r_p$  is the radius of a cylindrical pore. Note that by definition the radius of curvature of a concave surface is negative, hence, there is a pressure decrease in the liquid phase.

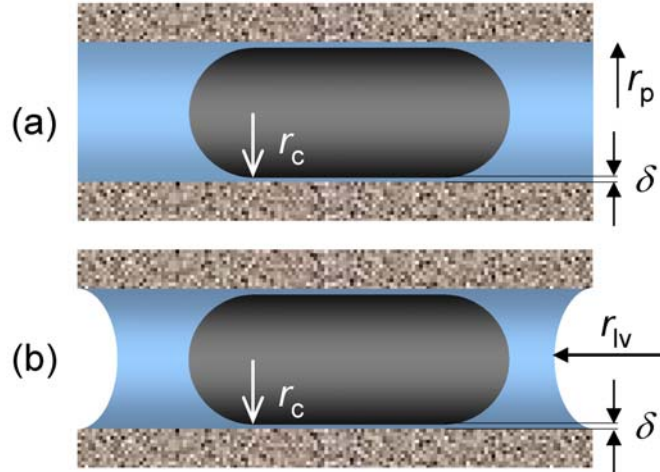


Figure 1: Liquid–vapor and crystal–liquid interface in a saturated (a) and unsaturated (b) porous material with cylindrical pore geometry;  $r_p$  is the pore radius,  $r_c$  is the radius of the cylindrical crystal, and,  $\delta = r_p - r_c$  is the thickness of the liquid film between the pore wall and the crystal.

In contrast, for a convex interface such as in solution droplets there is a pressure increase in the liquid. Assuming that the liquid is perfectly wetting the pore wall (i.e.  $\theta = 0$ ), which is a reasonable assumption for water in building materials, the Laplace law simplifies to  $\Delta p = -2\gamma_{lv}/r_p$ . For a pore radius of 5 nm, this yields a pressure of  $-29$  MPa in the liquid phase.

## 2.2 Vapor–liquid equilibrium

Here, we follow the treatment in our previous work [5]. The standard states for pure solid phases and water are unit activity at any temperature and pressure. For the aqueous species other than  $\text{H}_2\text{O}$ , the standard state is unit activity in a hypothetical one molal ideal solution referenced to infinite dilution at any temperature and pressure. Then, equilibrium between water vapor and liquid water in an aqueous solution requires equality of the chemical potentials in the liquid phase ( $\mu_l$ ) and in the gas phase ( $\mu_g$ ). The chemical potentials of liquid water and water vapor are given by

$$\mu_l = \mu_l^\circ + RT \ln a_w = \mu_g = \mu_g^\circ + RT \ln(p_w/p_w^\circ) \quad (2)$$

where  $a_w$  is the water activity of the solution,  $p_w$  is the water vapor partial pressure over the solution,  $p_w^\circ$  is the saturation vapor pressure and  $R$  and  $T$  are the gas constant and the absolute temperature, respectively. For a bulk sample of pure water at equilibrium we obtain  $a_w = 1$  and  $p_w = p_w^\circ$ . In the case of a salt solution at equilibrium, the water activity equals the ratio  $p_w/p_w^\circ$  which, by definition, is the relative humidity, RH.

For the chemical potential of liquid water under the reduced pressure  $p_l$  we obtain

$$\mu_l = \mu_l^\circ + RT \ln a_w + 2\gamma_{lv}\bar{V}_w/r_{lv} \quad (3)$$

where  $\bar{V}_w$  is the partial molar volume of water in the solution. The pressure dependence of the partial volume of water is rather small and is neglected in this study. For more accurate calculations, an appropriate equation for the calculation of the pressure dependence may be found in reference [6]. In the derivation it is also assumed that  $a_w$  is not a function of pressure. Strictly, however,

$$d \ln a_w / dp = (\bar{V}_w - \bar{V}_w^\circ) \Delta p / RT \quad (4)$$

where  $\bar{V}_w^\circ$  is the molar volume of pure water. It has been shown [7] that the quantity  $(\bar{V}_w - \bar{V}_w^\circ)$  is very small even at high solute concentrations. Therefore, the pressure dependence of  $a_w$  can be neglected and  $\bar{V}_w$  in Eq. (3) may be replaced by  $\bar{V}_w^\circ$ . Values of the molar volume of water were taken from Kell [8].

Then, at equilibrium, the water vapor partial pressure over a solution in an unsaturated porous material is given by:

$$\ln(p_w/p_w^\circ) = \ln a_w + 2\gamma_{lv} \bar{V}_w^\circ / (r_{lv} RT) \quad (5)$$

Equation (5) yields the depression of the water vapor partial pressure due to the influence of both dissolved salts and the curvature of the liquid–vapor interface in small unsaturated pores. The influence of the solution composition on the water activity can be calculated by using the ion interaction model presented in the previous chapter [1] and in reference [9].

### 2.3 Solid–liquid equilibria

For the dissolution reaction of a salt of general composition  $M_{v_M} X_{v_X} \cdot v_0 H_2O$



the thermodynamic solubility product is given by

$$\ln K = v_M \ln m_M + v_X \ln m_X + v_M \ln \gamma_M + v_X \ln \gamma_X + v_0 \ln a_w \quad (7)$$

where  $m_M$ ,  $m_X$ ,  $\gamma_M$  and  $\gamma_X$  represent the molalities and activity coefficients of the cations and anions, respectively. There are two influences that affect the solubility of a salt in a mesoporous material. First, there is an influence of crystal size as discussed in detail in reference [4]. Second there is an influence of the reduced pressure in an unsaturated material. The influence of crystal size on the solubility product in a cylindrical pore as shown in Fig. 1a is given by [4]:

$$\ln K_r^{(0)} = \ln K_\infty^{(0)} + \frac{2\gamma_{cl} V_m}{r_c RT} \quad (8)$$

where  $K_r^{(0)}$  and  $K_\infty^{(0)}$  are the thermodynamic solubility products at standard pressure (0.1 MPa) of the crystal with radius  $r_c$  and an infinitely large crystal, respectively;  $\gamma_{cl}$  is the interfacial free energy of the crystal–liquid interface and  $V_m$  is the molar volume of the solid.

The effect of pressure on the solubility is given by [10]:

$$\ln K_{\infty}^{(p)} = \ln K_{\infty}^{(0)} - \frac{\Delta \bar{V}^{\circ}}{RT} \Delta p + \frac{\Delta \bar{K}^{\circ}}{RT} (\Delta p)^2 \quad (9)$$

where  $K_{\infty}^{(p)}$  is the thermodynamic solubility product at pressure  $p$  and  $\Delta \bar{V}^{\circ}$  and  $\Delta \bar{K}^{\circ}$  are the changes in molar volume and molar compressibility of the dissolution reaction at 0.1 MPa. For example, the change in molar volume for the dissolution reaction (6) is given by

$$\Delta \bar{V}^{\circ} = \sum_i \bar{V}_i^{\circ} + \nu_0 \bar{V}_w^{\circ} - V_m \quad (10)$$

where  $\bar{V}_i^{\circ}$  are the partial molar volumes of the ions  $i$  at infinite dilution. An analogous expression holds for the change of standard compressibility. Combining Eqs. (8) and (9), yields an expression for the thermodynamic solubility product of a small crystal at pressure  $p$ :

$$\ln K_r^{(p)} = \ln K_{\infty}^{(0)} + \frac{2\gamma_{lc} V_m}{r_c RT} - \frac{\Delta \bar{V}^{\circ}}{RT} \Delta p + \frac{\Delta \bar{K}^{\circ}}{RT} \Delta p^2 \quad (11)$$

The calculation of freezing temperatures of salt solutions using the ion interaction model was described in detail in reference [11]. The equilibrium constant in a bulk solution is given by:

$$\ln K_{\infty} = a_w \quad (12)$$

Values of  $\ln K_{\infty}$  at various temperatures were taken from reference [12]. An expression analogous to Eq. (11) can then be used for the calculation of freezing temperatures in small pores where the change in molar volume and compressibility is given as the difference of the molar volumes and compressibilities of ice and liquid water [5]. This yields

$$\ln K_r^{(p)} = \ln K_{\infty}^{(0)} + \frac{2\gamma_{lc} V_{ice}}{r_c RT} - \frac{\bar{V}_w^{\circ} - V_{ice}}{RT} \Delta p + \frac{\bar{K}_w^{\circ} - K_{ice}}{RT} \Delta p^2 \quad (13)$$

where  $V_{ice}$  and  $K_{ice}$  are the molar volume and compressibility of ice. However, the compressibilities of water and ice were neglected in the present treatment.

### 3. Calculations

#### 3.1 Liquid phase pressure and liquid–vapor equilibrium

The calculation of the liquid phase pressure in pore solutions requires values of the interfacial energy of the liquid–vapor interface  $\gamma_{lv}$ , i.e. the surface tension of the pore solutions. The available experimental surface tension data have been tabulated by Abramzon and Gaukhberg [13]. For most salts, the available data are quite scattered. The following very simple equation proved to be sufficient to reproduce most of the experimental data of  $\gamma_{lv}$  to within their respective uncertainties:

$$\gamma_{lv} = \gamma_{lv}^{\circ} + gm \quad (14)$$

Here,  $\gamma_{lv}^{\circ}$  is the interfacial tension of pure water,  $m$  is the molality of the solution and  $g$  is an empirical parameter that is determined from experimental data for each salt. The interfacial tension of pure water at various temperatures has been calculated from the equation proposed by Cini et al. [14]. For the calculations with NaCl(aq) a temperature independent value of  $g = 1.66 \pm 0.02 \text{ J}\cdot\text{kg}\cdot\text{m}^{-2}\cdot\text{mol}^{-1}$  was used. Figure 2 depicts the calculated liquid phase pressures as a function of pore size for pure water and NaCl solutions. It is obvious that there is only a rather small influence of the surface tension of the solution on the liquid phase pressure. Hence, for binary solutions, our very simple approach for the calculation of interfacial tensions appears to be appropriate. For multicomponent systems, more complicated equations may be used such as, for example, provided in references [15] or [16].

The equilibrium of a salt solution of any composition in a porous material and the water vapor in the surrounding air can be treated using Eq. (5). For a bulk sample of pure water, i.e.  $\text{RH} = a_w = 1$ , it follows from Eq. (5) that the liquid–vapor interface is flat (i.e.  $r_{lv} = \infty$ ). For water in a small cylindrical pore, the curvature of the liquid–air interface increases with decreasing RH. The maximum curvature is reached if  $r_{lv} = -r_p$ ; any further decrease in RH will then cause the complete evaporation of the pore. In other words, if the relative humidity exceeds the critical value corresponding to the maximum curvature, capillary condensation occurs. Similar arguments apply to a salt solution in a small pore. In this case however, the water activity is lower and a flat surface is reached at a lower RH, namely at  $\text{RH} = a_w$ .

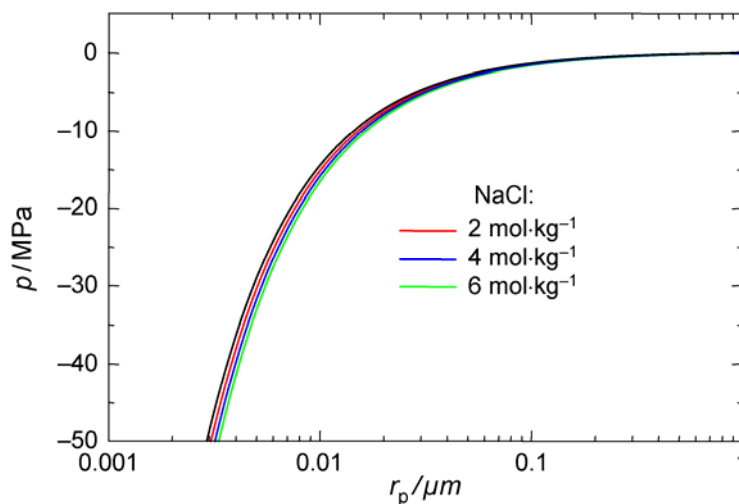


Figure 2: Liquid phase pressure as a function of pore size for pure water and NaCl solutions with molalities  $2 \text{ mol}\cdot\text{kg}^{-1}$ ,  $4 \text{ mol}\cdot\text{kg}^{-1}$  and  $6 \text{ mol}\cdot\text{kg}^{-1}$ .

### 3.2 Solubility of NaCl in mesoporous materials

It follows from Eq. (8) that there is an increase in solubility with decreasing crystal size. Therefore, salt solubilities in a saturated mesoporous material are higher than in a macroporous material. This is the theoretical basis of the equilibrium crystallization pressure that is generated by crystals that are confined in very small pores [4,17,18]. The additional influence of pressure in an unsaturated material is controlled by the change in molar volume and compressibility. Both, the values of  $\Delta\bar{V}^\circ$  and  $\Delta p$  are negative resulting in a solubility decrease at low pressure. Since the values of  $\Delta\bar{K}^\circ$  are also negative, it is expected that the solubility increase is less pronounced at very low pressures, i.e. in very small pores. A comparison of the two competing influences, i.e. crystal size and low pressure, on the solubility of NaCl is illustrated in Fig. 3.

In these calculations, a value of the molar volume of NaCl of  $27.02 \text{ cm}^3 \cdot \text{mol}^{-1}$  was used. A compilation of the molar volumes of other salt minerals relevant to building materials is provided in reference [19]. Values of the partial molar volumes of the ions  $i$  at infinite dilution were taken from our density model [1]. Values of the partial molar compressibilities at infinite dilution were taken from Millero [10]. There is a lack of reliable data for the compressibilities of the solid phases. However, compressibilities of solids are typically low relative to the partial compressibilities of the respective ions at infinite dilution [20]. Therefore, we have neglected the compressibilities of the solid phases yielding a value of  $-0.047 \text{ cm}^3 \cdot \text{mol}^{-1} \cdot \text{MPa}^{-1}$  for the change of the compressibility in the dissolution reaction of halite (NaCl).

The crystal size influence is largely controlled by the value of the crystal–liquid free energy  $\gamma_c$ . Unfortunately, no reliable experimental data of interfacial energies are available. In the case of NaCl(cr), we have adopted the value of  $\gamma_c = 30 \text{ mJ} \cdot \text{m}^{-2}$  given by Wu and Nancollas [21]. These authors also discuss the difficulties in the measurement of interfacial energies. The shaded area in Fig. 3a indicates the range of uncertainty in the solubility product that arises from an arbitrarily estimated uncertainty in the  $\gamma_c$  value of  $\pm 20 \text{ mJ} \cdot \text{m}^{-2}$ . This confirms the rather strong influence of the interfacial energy on the solubilities of very small crystals. There is a strong decrease of the NaCl solubility with decreasing pressure in small pores of unsaturated materials (Fig. 3b). As expected, the influence of compressibility is only significant at very low pressure, i.e. in very small pores.

Figure 4 depicts the combined influence of crystal size and the reduced liquid phase pressure in an unsaturated material, again calculated with different values of  $\gamma_c$ . The activity coefficients and water activities required for the calculation of solubilities were taken from the electrolyte solution model presented in the previous chapter [1,9]. The thickness of the solution film was assumed as  $\delta = 0.5 \text{ nm}$ . The very small influence of pressure on the activity coefficients of NaCl(aq) and the water activity were neglected.

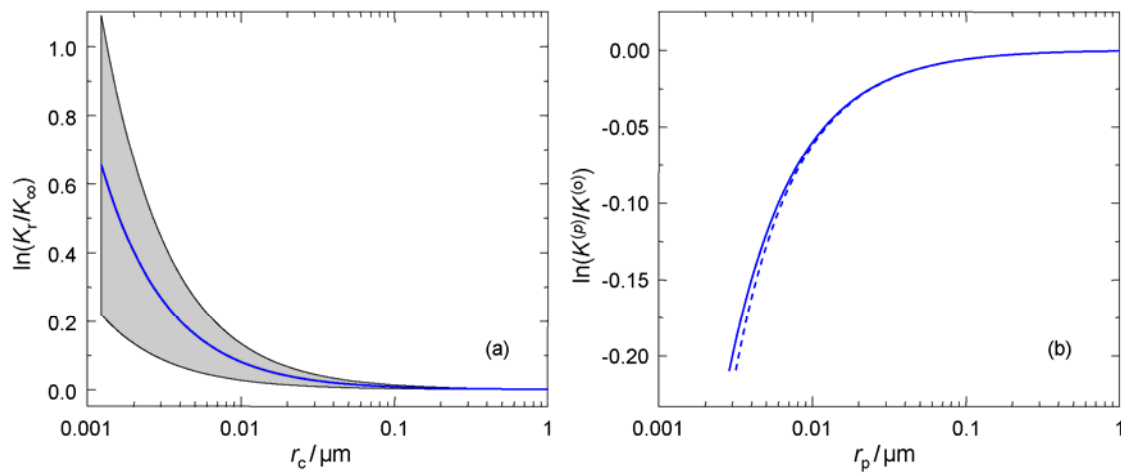


Figure 3: Solubility of NaCl in mesoporous materials (25 °C): (a) influence of crystal size in a saturated material at 0.1 MPa calculated with  $\gamma_c = 30 \text{ mJ}\cdot\text{m}^{-2}$  (the shaded area indicates the influence of an uncertainty in this value of  $\pm 20 \text{ mJ}\cdot\text{m}^{-2}$ ); (b) influence of reduced pressure in small pores of an unsaturated material with (—) and without (---) inclusion of the compressibility term.

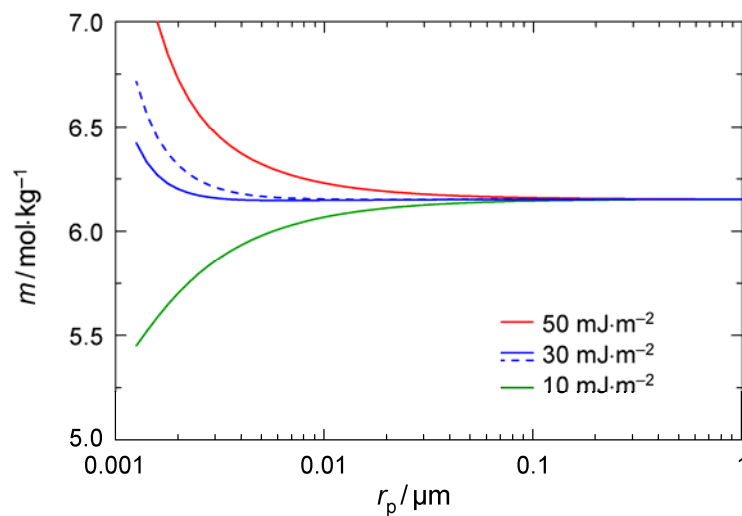


Figure 4: Solubility of NaCl as a function of pore size in mesoporous materials at 25 °C; with the exception of the dashed blue curve, all solubilities were calculated with the compressibility term in Eq. (11) included.

It is obvious from Fig. 4 that the pressure effect and the crystal size effect partly compensate each other. Even assuming significantly different values of  $\gamma_c$ , the influence on the solubility of NaCl crystals does not exceed about 10% down to pore radii of about 2 nm.

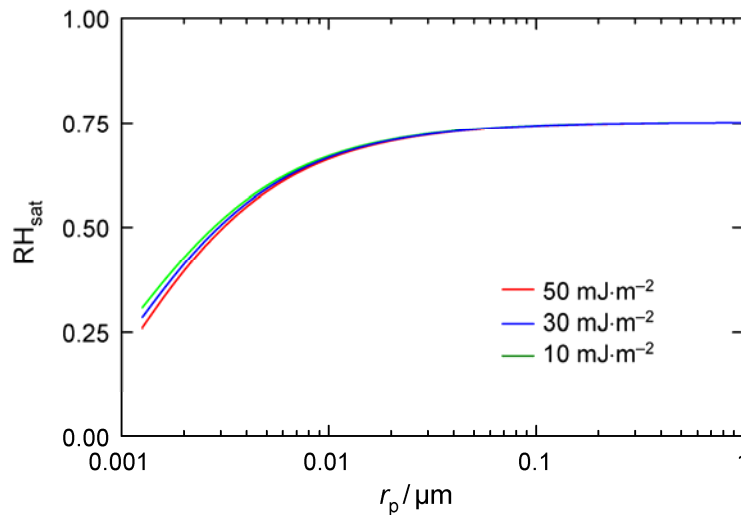


Figure 5: Saturation humidities  $RH_{\text{sat}}$  of saturated solutions of NaCl in unsaturated porous material at 25 °C; all calculations with inclusion of compressibility term.

More important than the solubility of NaCl is the saturation humidity, i.e. the relative humidity of the surrounding air that is in equilibrium with the saturated solution. Only if the relative humidity drops below the saturation humidity, the respective salt will crystallize out. Hence, no crystallization damage can occur at relative humidities above the saturation humidity. Figure 5 depicts the relative humidities in equilibrium with saturated NaCl solutions as a function of pore size. Using Eq. (5), calculations were carried out for the saturated solutions at different pore sizes as shown in Fig. 4. The water activities required in Eq. (5) were calculated with the electrolyte solution model [9]. It is obvious that there is a strong influence of pore size on the saturation humidities. Due to the curvature of the interface between the saturated solution and the air there is a substantial decrease in the saturation humidities. Sodium chloride in an unsaturated mesoporous material crystallizes at lower relative humidities than in macroporous materials. For example, a saturation humidity of 59% RH is calculated for an unsaturated cylindrical pore with a pore diameter of 10 nm, a value much lower than the value of 75.3% in bulk solutions. Figure 5 also shows that the uncertainty in the values of the interfacial energy of NaCl crystals that caused some scatter in the calculation of the solubilities in small pores is less critical in the calculation of the saturation humidity.

There are no experimental data of saturation humidities in mesoporous materials available that could be used to validate these model predictions. However, experimental data are available for the deliquescence humidities of nanosized aerosol particles [22,23]. Aerosol particles play a fundamental role in the microphysics of clouds. They provide heterogeneous nucleation sites for the formation of droplets. Water soluble aerosols such as NaCl can deliquesce to form saturated solutions in the form of small droplets that play an important role in forming haze and clouds and can act as sites for heterogeneous chemical reactions. Also, the hygroscopic growth of particles has important consequences for the predicted atmospheric radiative transfer of aerosols and their effect on climate.

The deliquescence of aerosol nanoparticles and the calculation of solubilities in nanosized droplets is a problem similar to the calculation of solubilities in small capillaries. In both cases there is a convex crystal–liquid interface. In droplets however, the curvature of the vapor–liquid interface is convex while this interface is concave in the case of a wetting fluid in small capillaries. For a convex interface,  $r_{lv}$  is positive resulting in a pressure increase in aerosol droplets with decreasing droplet size. Using the present model, solubilities and saturation humidities of NaCl in small droplets have been calculated and compared to experimental values [22,23]. Due to the convex interface, the deliquescence humidities are higher than for large crystals. In all cases, our calculations agree with the experimental values to within their stated uncertainty and correctly predict an increase in the deliquescence for small particle sizes. For example, for a 10 nm sized NaCl particle a deliquescence humidity of 84.8% is predicted. Note that the deliquescence of a particle in a small pore of the same size (10 nm diameter) was calculated at 59% RH. Finally, the agreement of the present calculations with the experimental data is significantly better than earlier model calculations of Mirabel et al. [24] as well as Russel and Ming [25].

### 3.3 Freezing temperatures

Calculations of freezing temperatures in bulk electrolyte solutions and in saturated and unsaturated porous materials have been reported earlier [5,11]. As an example, Fig. 6 depicts calculated freezing temperatures in bulk NaCl solutions and in NaCl pore solutions of a saturated mesoporous material in comparison to available experimental data [26,27,28,29]. In the calculations cylindrical pore geometry was assumed. The thickness of the unfrozen liquid film was assumed as  $\delta = 1$  nm. Molar volumes of supercooled water were taken from Kell [8] while the molar volume of ice was assumed to be independent of temperature ( $V_s = 19.65 \text{ cm}^3 \text{ mol}^{-1}$ ). Values of the ice–liquid water interfacial energy were taken from Brun et al. [28] and interfacial tensions and water activities of NaCl solutions were calculated as described before.

There is excellent agreement between experimental and calculated freezing temperatures in bulk solutions. It should be noted however, that freezing temperatures were used to determine the model parameters in the electrolyte solution model [9]. The pore size dependence of the freezing temperatures curves in Fig. 6 indicate that in pores larger than about 10 nm the freezing temperature depression is largely controlled by the presence of dissolved NaCl. In smaller pores the freezing temperature rapidly decreases mainly as a result of the small size of the ice crystals in these pores, i.e. the influence of the interfacial energy of the crystal–liquid interface. Also shown in Fig. 6b are experimental freezing temperatures of pure water in mesoporous materials [27–29].

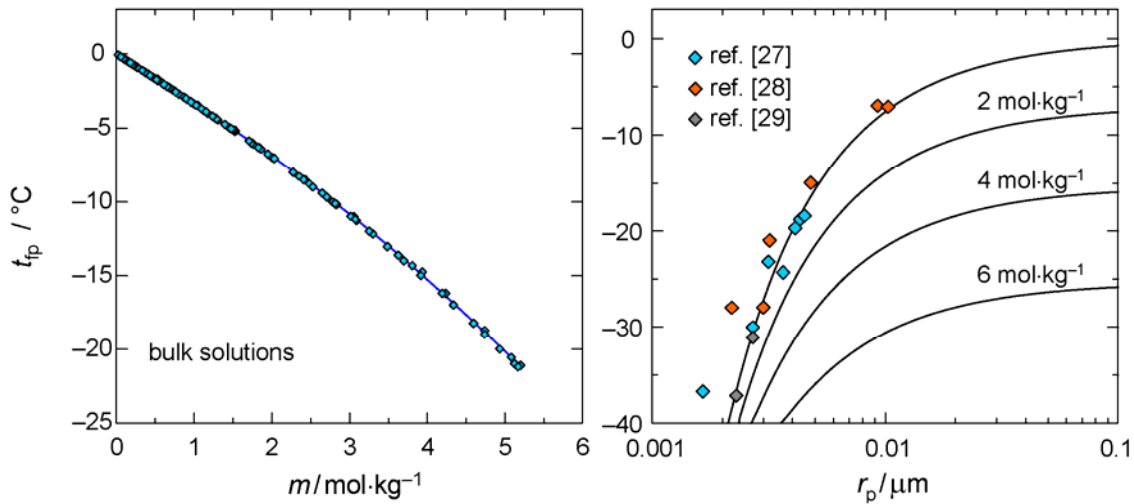


Figure 6: Freezing temperatures in NaCl solutions: (a) freezing temperatures in bulk solutions (symbols represent experimental data [26]); (b) freezing temperatures in saturated porous materials of pure water and NaCl solutions with  $2 \text{ mol}\cdot\text{kg}^{-1}$ ,  $4 \text{ mol}\cdot\text{kg}^{-1}$  and  $6 \text{ mol}\cdot\text{kg}^{-1}$  (symbols are experimental for pure water [27–29]).

Though these data are somewhat scattered, there is reasonable agreement with the calculated freezing temperatures. It has been shown in reference [5] that the pressure decrease in the liquid phase of unsaturated pores causes a minor increase in the freezing temperature in comparison to a saturated material. The resulting freezing temperature curves in unsaturated mesoporous materials are very similar to those shown in Fig. 6b. This is due to the fact that the difference in the molar volumes of liquid water and ice entering the second term on right-hand side of Eq. (13) is small.

#### 4. Conclusions

Phase equilibria in mesoporous materials are affected by the curvature of the vapor–solution and the crystal–solution interfaces. Using Eqs. (5), (11) and (13) together with our model of the thermodynamic properties of bulk solutions, it is possible to predict phase equilibria in small pores. The parameters that are required in addition to the models presented in the previous chapter [1], are the surface tensions of salt solutions, the crystal–liquid interfacial energies of the solid phases and the ionic partial molar compressibilities at infinite dilution. As long as calculations are only required for single salts, a very simple equation can be used to calculate surface tensions in salt solutions with sufficient accuracy. Somewhat more complicated equations will be required in future work with mixed salt solutions. Accurate experimental data for the crystal–liquid interfacial energies of the solid phases are not available, hence, these values have to be estimated using equations available in the literature. Fortunately, the test calculations for NaCl carried out in this study indicate that the uncertainty in the  $\gamma_{cl}$  values may not cause unacceptable large errors at realistic pore sizes.

The calculated solubilities imply that there is not such a strong change in solubilities of salts in very small pores. A partial compensation of the competing influences of crystal size and liquid phase pressure in unsaturated mesoporous materials is the main reason for this behavior. In contrast to the solubilities, the saturation humidities in unsaturated materials are strongly affected by the pore size, i.e. there is a significant decrease in the saturation humidity with decreasing pore size. It is important to note, that the uncertainties in the interfacial energies of the solids do not introduce large error in the calculation of the saturation humidities.

Finally, it has been shown that the same model equations can be used to predict the behavior of aerosol particles in atmospheric applications where a convex solution–vapor interface causes a pressure increase in solution droplets. The resulting increase in the saturation or deliquescence humidities is accurately predicted by the present model.

## 5. References

- [1] Linnow K., Steiger M.: Modeling the properties of pore solutions in porous building materials. This volume.
  - [2] Steiger M.: Salts in porous materials: Thermodynamics of phase transitions, modeling and preventive conservation. *Restoration of Buildings and Monuments* 11, pp. 419–431, 2005.
  - [3] Sing K. S. W., Everett D. H., Haul R. A. W., Moscou L., Pierotti R. A., Rouquerol J., Siemieniewska T.: Reporting physisorption data for gas/solid system with special reference to the determination of surface area and porosity. *Pure & Applied Chemistry* 57, pp. 603–619, 1985.
  - [4] Steiger M.: Crystal growth in porous materials:—II. The influence of crystal size. *Journal of Crystal Growth* 282, pp. 470–481, 2005.
  - [5] Steiger M.: Freezing of salt solutions in small pores. In: M.S. Konsta-Gdoutos (ed.): *Measuring, Monitoring and Modelling Concrete Properties*, Springer, Dordrecht, pp. 661–668, 2006.
  - [6] Mercury L., Tardy Y.: Negative pressure of stretched liquid water. *Geochimica et Cosmochimica Acta* 65, pp. 3391–3408, 2001.
  - [7] Monnin C.: The influence of pressure on the activity coefficients of the solutes and the solubility of minerals in the system Na–Ca–Cl–SO<sub>4</sub>–H<sub>2</sub>O to 200 °C and 1 kbar, and to high NaCl concentration. *Geochimica et Cosmochimica Acta*, 54, pp. 3265–3282, 1990.
  - [8] Kell G. S.: Effects of isotopic composition, temperature, pressure, and dissolved gases on the density of liquid water. *Journal of Physical and Chemical Reference Data* 6, pp. 1109–1131, 1977.
  - [9] Steiger M., Kiekbusch J., Nicolai A.: An improved model incorporating Pitzer's equations for calculation of thermodynamic properties of pore solutions implemented into an efficient program code. *Construction and Building Materials* 22, pp. 1841–1850, 2008.
  - [10] Millero F. J.: The effect of pressure on the solubility of minerals in water and seawater. *Geochimica et Cosmochimica Acta* 46, pp. 11–22, 1982.
  - [11] Steiger M.: Influence of salts on the freezing temperature of water: implications on frost damage to porous materials. In: D. Kwiatkowski, R. Löfvendahl (eds.): *Proceedings of the 10th International Congress on Deterioration and Conservation of Stone*, ICOMOS, Stockholm, 2004, pp. 179–186, 2004.
  - [12] Klotz I. M., Rosenberg R. M.: *Chemical thermodynamics, basic theory and methods*. Benjamin/Cummings, Menlo Park CA, 3rd ed., pp. 374–378, 1972.
-

- [13] Abramzon A. A., Gaukhberg R. D.: Surface tension of salt solutions. *Russian Journal of Applied Chemistry* 66, pp. 1139–1146, pp. 1315–1320, pp. 1473–1480, 1993.
- [14] Cini R., Loglio G., Ficalbi A.: Temperature dependence of the surface tension of water by the equilibrium ring method. *Journal of Colloid and Interface Science* 41, pp. 287–297, 1972.
- [15] Li Z., Lu B. Z.-Y.: Surface tension of aqueous electrolyte solutions at high concentrations – representation and prediction. *Chemical and Engineering Science* 56, pp. 2879–2888, 2001.
- [16] Hu Y.-F., Lee H.: Prediction of the surface tension of mixed electrolyte solutions based on the equation of Patwardhan and Kumar and the fundamental Butler equation. *Journal of Colloid and Interface Science* 269, pp. 442–448, 2004.
- [17] Everett D. H.: The thermodynamics of frost damage to porous solids. *Transactions of the Faraday Society* 57, pp. 1541–1551, 1961.
- [18] Scherer G. W.: Crystallization in pores. *Cement and Concrete Research* 29, 1347–1358.
- [19] Steiger M.: Total volumes of crystalline solids and salt solutions. In: Price C. A. (ed.), *An expert chemical model for determining the environmental conditions needed to prevent salt damage in porous materials*. European Commission, Research Report 11, pp. 53–63, 2000.
- [20] Marion G.M., Kargel J. S., Catling D. C., Jakubowski S. D.: Effects of pressure on aqueous chemical equilibria at subzero temperatures with applications to Europa. *Geochimica et Cosmochimica Acta* 69, pp. 259–274, 1982.
- [21] Wu W., Nancollas G. H.: Determination of interfacial tension from crystallization and dissolution data: a comparison with other methods. *Advances in Colloid and Interface Science* 79, pp. 229–279, 1999.
- [22] Hämeri K., Laaksonen A., Väkevä M., Suni T.: Hygroscopic growth of ultrafine sodium chloride particles. *Journal of Geophysical Research* 106, pp. 20749–20757, 2001.
- [23] Biskos G., Malinowski A., Russell L. M., Buseck P. R., Martin S. T.: Nanosize effect on the deliquescence and the efflorescence of sodium chloride particles. *Aerosol Science and Technology* 40, pp. 97–106, 2006.
- [24] Mirabel P., Reiss H., Bowles R. K. : A theory for the deliquescence of small particles. *Journal of Chemical Physics* 113, pp. 8200–8205, 2000.
- [25] Russel L. M., Ming Y.: Deliquescence of small particles. *Journal of Chemical Physics* 116, pp. 311–321, 2002.
- [26] Cohen-Adad R., Lorimer P. W: Alkali metal and ammonium chlorides in water and heavy water (binary systems). *Solubility Data Series*, International Union of Pure and Applied Chemistry, Pergamon Press, Oxford, pp. 80–84, 1991
- [27] Schreiber A., Ketelsen I., Findenegg G. H.: Melting and freezing of water in ordered mesoporous silica materials. *Physical Chemistry and Chemical Physics* 3, pp. 1185–1195, 2001.
- [28] Brun M., Lallemand A., Quinson J.-F., Eyraud C.: A new method for the simultaneous determination of the size and the shape of pores: The thermoporometry. *Thermochimica Acta* 21, pp. 59–88, 1977.
- [29] Morishige K., Kawano K.: Freezing and melting of water in a single cylindrical pore: The pore-size dependence of freezing and melting behavior. *Journal of Chemical Physics* 110, pp. 4867–4872,
-